Tetrahedron 65 (2009) 8869–8878

Contents lists available at ScienceDirect

Tetrahedron

journal homepage: www.elsevier.com/locate/tet

# Origin of enantioselectivity with heterobidentate sulfide-tertiary amine ($sp^3$) ligands in palladium-catalyzed allylic substitution

Jun-Long Niu, Min-Can Wang *, Pei-Pei Kong, Qing-Tao Chen, Yu Zhu, Mao-Ping Song *

*Department of Chemistry, Henan Key Laboratory of Chemical Biology and Organic Chemistry, Zhengzhou University, Zhengzhou, Henan 450052, PR China*

ARTICLE INFO

*Article history:*
Received 29 May 2009
Received in revised form 12 August 2009
Accepted 14 August 2009
Available online 19 August 2009

*Keywords:*
Aziridine
Allylic substitution
Palladium
Intermediate
Trans effect

ABSTRACT

A series of new chiral heterobidentate sulfide-tertiary amine ($sp^3$) ligands **3a–c**, **6** were readily prepared from cheap and easily available (*R*)-cysteine and L-(+)-methionine. A Pd-catalyzed asymmetric allylic alkylation of 1,3-diphenyl-2-propenyl acetate with dimethyl malonate was used as a model reaction to examine the catalytic efficiencies of these aziridine sulfide ligands, and ligand **3b** afforded the enantioselectivity of up to 91% ee. The origin of enantioselectivity for heterobidentate sulfide-tertiary amine ($sp^3$) ligands was first rationalized based on X-ray crystallographic data, and NMR spectroscopic data for relevant intermediate palladium allylic complexes. Our results demonstrated that the sulfur atom was a better π-allyl acceptor than the nitrogen atom for heterobidentate sulfide-tertiary amine ($sp^3$) ligands, and the steric as well electronic properties of the palladium allylic complexes were crucial for the enantioselectivity.



## 1. Introduction

Enantioselective reactions based on transition-metal catalyzed allylic substitutions have been investigated with great intensity due to the synthetic potential of the products of these types of reactions.[1] Since the first palladium-catalyzed enantioselective allylic substitution process was described by Trost in 1977,[2] many types of the efficient homo- and hetero-donor chiral ligands such as N,N-,[3] P,P-,[4] N,P-,[3h,5] N,S-,[5i,5h,6,19] and P,S-types[7] have been exploited in this asymmetric carbon–carbon bond-forming reaction, affording excellent enantiomeric excesses.[8] In comparison to homobidentate ligands used in palladium-catalyzed allylic substitution reactions, heterobidentate ligands allow more permutation, and provide selectivity control since the different electronic properties of the two heterodonor atoms may lead to the unsymmetrical binding of the two atoms to palladium in the intermediate π-complex.[9] As a result, the nucleophilic attack takes place at the allylic terminal carbon atom *trans* to the more powerful π-acceptor. In N,P- and P,S-bidentate ligands, the P atom is regarded as the more powerful π-acceptor. In N,S-bidentate ligands that contain $sp^2$ nitrogen atoms such as thioether-imines,[10] thioether-oxazolines,[5h,11] thioether-pyridines,[12] some examples showed that the nitrogen atom was the more powerful π-acceptor,[10a,c] while in other examples sulfur atom was the more powerful π-acceptor.[5h,11g,12b] Unfortunately, only a few examples regarding N,S-bidentate ligands that contain $sp^3$ nitrogen atoms were reported in this study.[13] Furthermore, there are no structural data that demonstrate which atom of the N ($sp^3$), S-bidentate ligands, N atom or S atom, is the better π-acceptor in the intermediate palladium–π-complex, and hence the origin of the pattern of enantioselectivity observed for heterobidentate sulfide-tertiary amine ($sp^3$) ligands is also unclear in palladium-catalyzed allylic substitution reactions.

In recent years,[14] we have been exploring the synthesis of chiral ferrocenyl nitrogen heterocycle ligands and their use in catalytic asymmetric synthesis. Our results demonstrated that the three- and four-membered heterocycle-based backbone was a good chiral unit for the catalytic asymmetric reaction. Moreover, it was discovered that the replacement of the phenyl group on the nitrogen atom of heterocycle-based skeleton by a ferrocenyl unit led to a dramatic improvement in the enantioselectivity. In order to examine the generality of these findings, in this article, we present our results on synthesis of new enantio-pure *N*-ferrocenylmethyl aziridine sulfide ligands **3a–c**, **6** and their application in palladium-catalyzed allylic substitution reaction. The origin of the pattern of enantioselectivity for heterobidentate sulfide-tertiary amine ($sp^3$) ligands was first rationalized by the X-ray diffraction and solution NMR studies of the intermediate palladium–π-complex.

## 2. Results and discussion

### 2.1. Synthesis of chiral ligands

The chiral ligands **3a–c** were readily obtained from the reaction of ferrocenecarboxaldehyde with (*R*)-cysteine (Scheme 1). (*R*)-Cysteine

* Corresponding authors. Tel./fax: +86 371 67769024.
*E-mail addresses:* wangmincan@zzu.edu.cn (M.-C. Wang), mpsong9350@zzu.edu.cn (M.-P. Song).

0040-4020/$ – see front matter © 2009 Elsevier Ltd. All rights reserved.
doi:10.1016/j.tet.2009.08.037

was first condensed with ferrocenecarboxaldehyde in EtOH in the presence of NaOAc, then reduced by $NaBH_4/I_2$, to afford the disulfide amino alcohols **1**.[15] Disulfides **1** were reduced with $NaBH_4$, and then alkylated, to give thioethers **2**.[16] Attempts to cyclise **2** via the methanesulfonyl chloride or the *p*-toluenesulfonyl chloride using triethylamine afforded products **3** in very poor yields.[17] Treatment of **2** with triphenylphosphine and tetrachloromethane in $CH_3CN$ at room temperature for 19 h,[18] however, led to the desired aziridine sulfides **3** in reasonable yield.

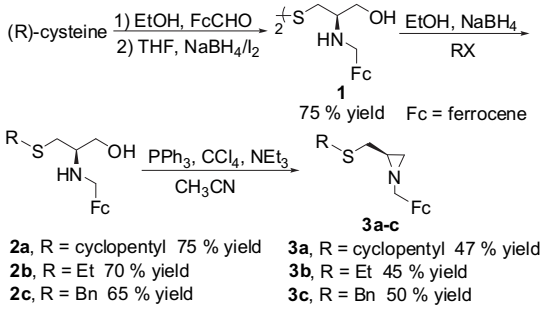


**Scheme 1.** Synthesis of chiral aziridine-thioether ligands **3a–c**.

Williams et al.[19] reported that the longer tether length between the donor atoms, which coordinate palladium may bring the asymmetric environment closer to the allyl species during the reaction, and provide the greater enantioselectivity. In order to explore the benefits of a longer tether length, we synthesized the aziridine sulfide **6** with the longer tether length between N and S atoms compared to ligands **3**. The chiral aziridine sulfide **6** was readily prepared from L-(+)-methionine in a straightforward three steps synthetic route (Scheme 2). Reduction of L-(+)-methionine with $NaBH_4/I_2$ afforded readily the amino alcohol **4** containing a thioether linkage.[15b] Amino alcohol **4** was converted into ferrocenyl amino alcohol **5** by the condensation of **4** with ferrocenecarboxaldehyde in MeOH, followed by $NaBH_4$ reduction.[14d] The compound **5** was cyclized to yield the aziridine sulfide **6** by the same procedure used in the synthesis of **3**.

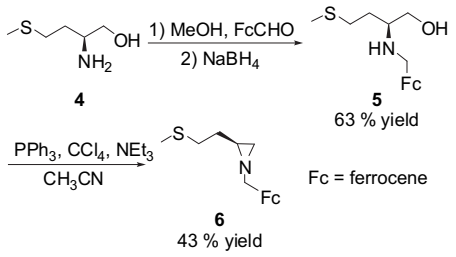


**Scheme 2.** Synthesis of chiral aziridine-thioether ligand **6**.

## 2.2. Asymmetric allylic alkylation

To examine the catalytic efficiencies of **3a–c**, **6** as chiral ligands in palladium-catalyzed allylic substitution, the asymmetric alkylation of 1,3-diphenyl-2-propenyl acetate with the nucleophile derived from dimethyl malonate was chosen as model reaction. The nucleophile was generated either from dimethyl malonate (DMM) and sodium hydride or from dimethyl malonate in the presence of N,O-bis-(trimethylsilyl) acetamide (BSA). The absolute configuration of the major enantiomer was determined to be S in all cases by the optical rotation and the comparison of peaks in chiral HPLC analysis.[20]

It was reported that the level of asymmetric induction was greatly dependant upon the base, temperature, solvent, and the loading of ligands in palladium-catalyzed allylic substitution reactions. Using NaH as base, we first examined the effects of temperature, solvent, and the loading of ligands on reaction yields and enantioselectivies, and the results were summarized in Table 1. Lowering the reaction temperature from room temperature (20–25 °C) to 0 °C resulted in a big increase in both the enantioselectivities from 75% to 86% and yields from 34% to 94% (Table 1 entry 1 vs 2) in THF in the presence of 2.5 mol % **3a**. A decrease in enantioselectivity and yield was observed when the reaction was carried out in $CH_2Cl_2$ at 0 °C (Table 1, entry 3). Using toluene as solvent, instead of $CH_2Cl_2$, led to an improvement in enantioselectivity and yield (Table 1, entry 4).

**Table 1**
Asymmetric allylic alkylation of 1,3-diphenyl-2-propenyl acetate using ligands **3a–c**, **6** and sodium hydride procedure[a]

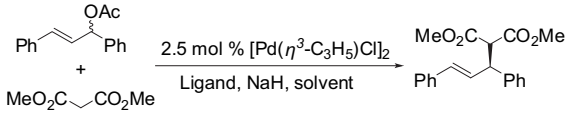


| Entry | Ligand | Pd/L | Solvent | Temp [°C] | Time [h] | Yield [%][b] | ee [%][c] | Config[d] |
|---|---|---|---|---|---|---|---|---|
| 1 | **3a** | 1:1 | THF | rt | 48 | 34 | 75 | *S* |
| 2 | **3a** | 1:1 | THF | 0 | 48 | 94 | 86 | *S* |
| 3 | **3a** | 1:1 | $CH_2Cl_2$ | 0 | 48 | 86 | 82 | *S* |
| 4 | **3a** | 1:1 | Toluene | 0 | 48 | 96 | 87 | *S* |
| 5 | **3a** | 1:2 | Toluene | 0 | 32 | 99 | 84 | *S* |
| 6 | **3a** | 1:3 | Toluene | 0 | 32 | 99 | 82 | *S* |
| 7 | **3a** | 1:4 | Toluene | 0 | 32 | 99 | 82 | *S* |
| 8 | **3b** | 1:1 | Toluene | 0 | 48 | 87 | 83 | *S* |
| 9 | **3c** | 1:1 | Toluene | 0 | 48 | 83 | 81 | *S* |
| 10 | **6** | 1:1 | Toluene | 0 | 48 | 98 | 50 | *S* |
| 11 | **6** | 1:4 | Toluene | 0 | 48 | 99 | 75 | *S* |

[a] Conditions: 2.5 mol % $[Pd(\eta^3\text{-}C_3H_5)Cl]_2$, 100 mol % 1,3-diphenyl-2-propenyl acetate, 250 mol % sodium dimethyl malonate.
[b] Isolated yield based on 1,3-diphenyl-2-propenyl acetate.
[c] Determined by HPLC (see Experimental Section).
[d] The absolute configuration of the product was assigned through comparison of the sign of specific rotations with literature data.[20]

The influence of the metal/ligand ratio was investigated for the range of 1:1, 1:2, 1:3, and 1:4 (with the amount of Pd held constant at 2.5 mol %, Table 1, entries 4–7). The reaction enantioselectivities decreased with the increase in the ligand/metal ratio. The 1:1 M ratio of $[Pd(\eta^3\text{-}C_3H_5)Cl]_2$ to **3a** proved to be the best condition, and provided higher enantioselectivity (Table 1, entry 4). The decrease in the enantioselectivity might be caused by a change in the coordination mode of the ligand to the Pd center when the ligand/metal ratio was increased. Similar phenomena were also observed in palladium-catalyzed allylic substitution reactions in the presence of the same type of chiral ligands.[13f]

The effect of the substituents on the sulfur atom on enantioselectivity was examined under the optimized conditions. When R was an ethyl group or a benzyl group, the asymmetric allylic substitution reaction gave the allylic alkylation products with 83% ee, and 81% ee, respectively.

Recently, Braga et al.[13f] reported the same type of chiral ligands **7a** and **7b** for the palladium-catalyzed allylic substitution reactions under the same reaction condition, with the enantioselectivity of up to 85% ee, and 99% ee, respectively (Fig. 1). Comparison of our results (**3c**: 81% ee) with those (**7a**: 85% ee) of Braga et al. suggested that the hindrance of rigid, bulky ferrocenyl group, compared with a phenyl group, did not seem to play a decisive role in the enantioselectivity. Instead, the chiral ligand **7b** with an electron-withdrawing

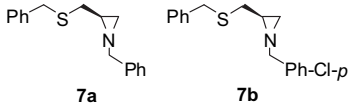


**Figure 1.** Ligands **7a** and **7b**.

substituent on benzene ring on the nitrogen atom afforded enantioselectivity of up to 99% ee. The results indicated also that the electronic effect played an important role in the enantioselectivity.

The chiral ligand **6** with the longer tether was also tested (Table 1, entries 10, and 11). However, in contrast with the ligand **3a**, increasing the ratio of ligand to palladium afforded an increase in enantioselectivity in the presence of **6** (Table 1, entry 11 vs 10). A possible explanation was that the ligand **6** formed six-membered ring chelate when bounds to a metal, and the complex of ligand **6** is less likely to ring-open compared with five-membered ring chelate, giving two monodentate complexes.[5e]

**Table 2**
Results of enantioselective allylic alkylation of 1,3-diphenyl-2-propenyl acetate using ligands **3a**–**c** and BSA procedure[a]

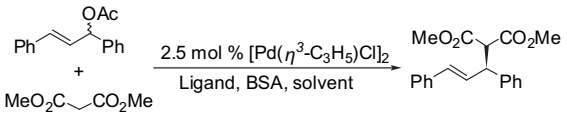


| Entry | Ligand | Pd/L | Base | Solvent | Temp [°C] | Time [h] | Yield [%][b] | ee [%][c] | Config[d] |
|---|---|---|---|---|---|---|---|---|---|
| 1 | **3b** | 1:1 | BSA/KOAc | THF | rt | 5 | 64 | 72 | *S* |
| 2 | **3b** | 1:1 | BSA | THF | rt | 48 | 95 | 91 | *S* |
| 3 | **3b** | 1:1 | BSA | THF | 0 | 48 | 93 | 85 | *S* |
| 4 | **3b** | 1:1 | BSA | $CH_3CN$ | rt | 48 | 99 | 80 | *S* |
| 5 | **3b** | 1:1 | BSA | $CH_2Cl_2$ | rt | 48 | 99 | 73 | *S* |
| 6 | **3b** | 1:1 | BSA | Toluene | rt | 48 | 99 | 75 | *S* |
| 7 | **3a** | 1:1 | BSA | THF | rt | 48 | 95 | 89 | *S* |
| 8 | **3c** | 1:1 | BSA | THF | rt | 48 | 94 | 78 | *S* |

[a] Conditions: 2.5 mol % $[Pd(\eta^3\text{-}C_3H_5)Cl]_2$, 10 mol % ligands, 100 mol % 1,3-diphenyl-2-propenyl acetate, 3 mol % KOAc, 300 mol % $CH_2(CO_2Me)_2$, 300 mol % BSA.
[b] Isolated yield based on 1,3-diphenyl-2-propenyl acetate.
[c] Determined by HPLC (see Experimental Section).
[d] The absolute configuration of the product was assigned through comparison of the sign of specific rotations with literature data.[20]

Then, we further examined the effects of base on the enantioselectivity and the reactivity. A soft anionic nucleophile (ketene silyl acetal, KSA) was generated from DMM in the presence of BSA and KOAc.[3e] The allylic alkylation reaction catalyzed by the chiral ligand **3b** proceeded smoothly to give the desirable product with 72% ee in 64% yield in the presence of a catalytic amount of potassium acetate (Table 2, entry 1). Much to our surprise, only in the presence of BSA, the chiral ligand **3b** could catalyze this transformation to afford the enantioselectivity of up to 91% ee and 95% yield (Table 2, entry 2). We attempted to decrease the reaction temperature further in order to have better enantioselectivity, but a decrease in both yield and enantioselectivity was observed when the reaction was performed at 0 °C (Table 2, entry 3). We also examined the effects of other solvent such as toluene, $CH_3CN$, and $CH_2Cl_2$ on reaction yields and enantioselectivities (Table 2, entries 4–6), and the results suggested that THF gave the best enantioselectivity. Under the optimized reaction conditions, chiral ligands **3a** and **3c** also gave high enantioselectivities with 89% ee, and 78% ee, respectively (Table 2, entries 7 and 8).

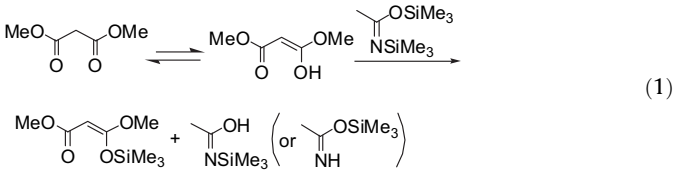


(1)

In previous reports on palladium-catalyzed enantioselective allylic substitution in the presence of BSA, an acetate salt such as KOAc frequently had to be added to this catalytic system in order to improve the reaction enantioselectivity. Aït-Haddou et al.[3e] proposed that BSA worked not only as a base, but also as a silylating agent for the dimethyl malonate salt to produce a ketene silyl acetal (KSA). Additionally, they confirmed this hypothesis by using ketene silyl acetal of dimethyl malonate under the same reaction conditions. Indeed, it was reported that ketene silyl acetals were successfully applied in palladium-catalyzed asymmetric allylic substitution as alternative nucleophiles to the 'harder' anionic species.[21] In the absence of KOAc, the allylic alkylation proceeded well under our conditions. Therefore, we assumed that in the absence of KOAc, BSA acted only as a silyating reagent of dimethyl malonate to generate a ketene silyl acetal, did not work as a base (Eq. 1).

## 2.3. Mechanistic considerations and proposals

According to the accepted mechanism, the palladium–allyl complex with *syn–syn* geometry formed after the oxidative addition of the racemic substrate is the key intermediate of the reaction. Frequently, this palladium–allyl complex isomerizes in solution, and gives two possible orientations (so-called *W*-type and *M*-type) for the π-allyl fragment with respect to the coordination plane defined by the Pd, N, and S atoms (Scheme 3). The sense and level of enantioselectivity observed will depend on the different reactivity of diastereomeric allyl complexes, their relative amounts, and/or on the site selectivity of the nucleophilic attack.[22]

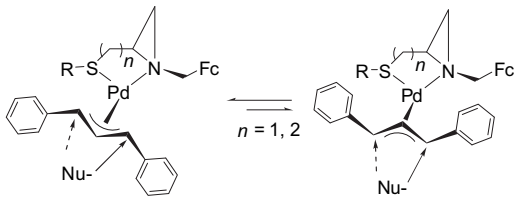


**8a.** *syn-syn* (M-type) **8b.** *syn-syn* (W-type)

**Scheme 3.** Possible models of the intermediate complexes.

Because of the different electronic characters of two coordination atoms of heterobidentate ligands, the bond length of the palladium–allyl terminus carbon trans to the more powerful π-acceptor atom will be longer, weaker, and hence more susceptible to cleavage as a result of nuceleophilic attack, called the trans effect. In other words, the nucleophile would preferentially attack the allylic system on the carbon possessing a greater positive charge character, i.e., on the carbon situated trans to the best π-acceptor. According to orientation of the palladium–allyl complex, the trans effect can explain the absolute configuration of products. For example, for the *W*-type configuration as the active catalyst species, if nitrogen is a more powerful π-acceptor than sulfur, the attack of nucleophile would occur at the allylic carbon atom trans to nitrogen, giving the *R* configuration product. However, if sulfur is the more powerful π-acceptor, the product with the *S* configuration would be obtained. Conversely, if the allylic unit adopts the *M*-type isomer, the result would be opposite to the above statement.

The mentioned-above structural data and/or information, such as the bond length and *W*/*M* configuration, the reactivity and relative amounts of intermediate, and/or on the site selectivity of the nucleophilic attack, could be revealed in the solid state by X-ray crystallography and in solution by NMR spectroscopy.

## 2.4. Synthesis and X-ray crystallographic studies of the intermediate complexes

X-ray crystallography of the chiral ligand–Pd–π-allyl intermediate complex can reveal the difference of bond distances

between palladium and allylic carbon termini as well as configuration of allyl moiety, and hence provide firm evidence for transition state model and more insight into the mechanism of chirality transfer. Therefore, the palladium–allylic complexes **9**–**11** were prepared from the bis[($\mu$-chloro)($\eta^3$-1,3-diphenylallyl)palladium(II)] and ligands **3a**, **3b**, and **6**, respectively (Eq. 2), in the presence of $AgSbF_6$ by slow evaporation a $CH_2Cl_2$/hexane solution.[23]

$$\text{Ligand} + [PdCl(PhC_3H_3Ph)]_2 \xrightarrow{AgSbF_6} \text{Complex} \quad (2)$$

**Ligand: 3a, 3b, 6** **Complex: 9, 10, 11**

The ORTEP drawings of complexes **9**, **10**, and **11** were given in Figures 2–4, respectively. A general feature of all the ionic Pd complexes is the unique configuration of the nitrogen atoms on

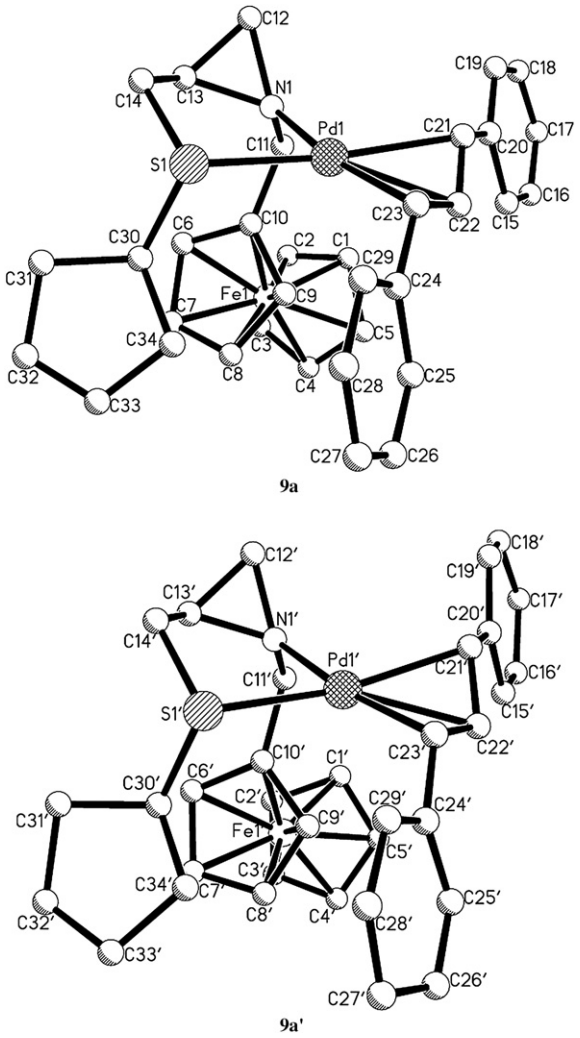


**Figure 2.** ORTEP drawing of the X-ray crystallographic structure and atom-numbering scheme of the two nonequivalent cations (**9a** and 9a′). Hydrogen atoms have been omitted for clarity. Selected bond lengths [Å] and angles [deg]: Pd(1)–N(1) 2.099(12), Pd(1)–S(1) 2.356(4), Pd(1)–C(21) 2.216(14), Pd(1)–C(22) 2.174(14), Pd(1)–C(23) 2.168(13), N(1)–Pd(1)–S(1) 85.3(4), N(1)–Pd(1)–C(21) 102.3(5), N(1)–Pd(1)–C(22) 133.2(5), N(1)–Pd(1)–C(23) 170.3(5), C(21)–Pd(1)–S(1) 166.9(4), C(22)–Pd(1)–S(1) 140.4(4), C(23)–Pd(1)–S(1) 103.6(4), C(22)–Pd(1)–C(21) 35.9(6), C(23)–Pd(1)–C(21) 68.2(6), C(23)–Pd(1)–C(22) 38.9(6), Pd(1′)–N(1′) 2.123(8), Pd(1′)–S(1′) 2.382(3), Pd(1′)–C(21′) 2.171(12), Pd(1′)–C(22′) 2.175(10), Pd(1′)–C(23′) 2.132(11), N(1′)–Pd(1′)–S(1′) 85.3(3), N(1′)–Pd(1′)–C(21′) 102.0(4), N(1′)–Pd(1′)–C(22′) 133.1(4), N(1′)–Pd(1′)–C(23′) 171.8(5), C(21′)–Pd(1′)–S(1′) 163.1(3), C(22′)–Pd(1′)–S(1′) 140.7(4), C(23′)–Pd(1′)–S(1′) 102.1(4), C(21′)–Pd(1′)–C(22′) 37.9(5), C(23′)–Pd(1′)–C(21′) 69.9(5), C(23′)–Pd(1′)–C(22′) 40.3(5).

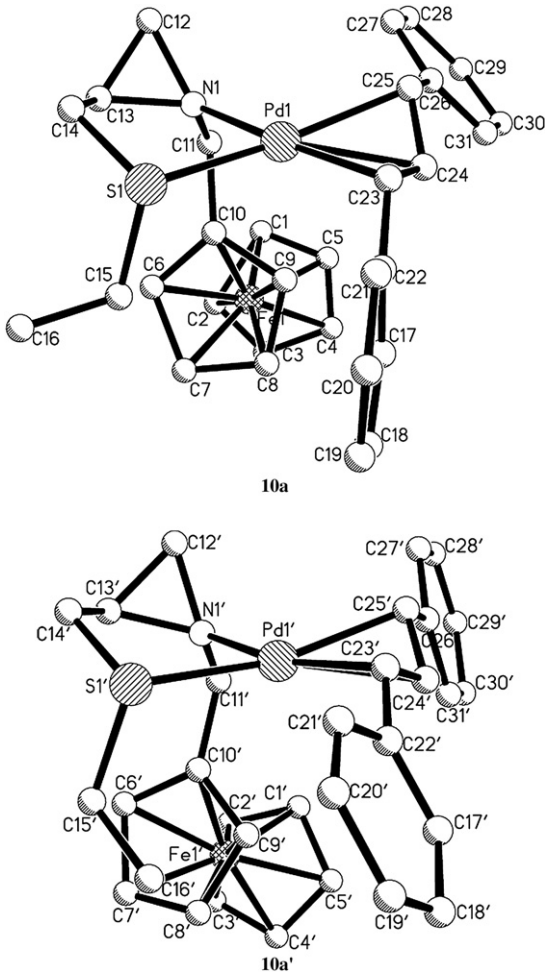


**Figure 3.** ORTEP drawing of the X-ray crystallographic structure and atom-numbering scheme of the two nonequivalent cations (**10a** and 10a′). Hydrogen atoms have been omitted for clarity. Selected bond distances [Å] and angles [deg]: Pd(1)–N(1) 2.150(6), Pd(1)–S(1) 2.355(3), Pd(1)–C(23) 2.136(13), Pd(1)–C(24) 2.155(13), Pd(1)–C(25) 2.197(14), N(1)–Pd(1)–S(1) 84.5(3), N(1)–Pd(1)–C(23) 174.8(5), N(1)–Pd(1)–C(24) 137.0(4), N(1)–Pd(1)–C(25) 106.7(5), C(23)–Pd(1)–S(1) 100.7(4), C(24)–Pd(1)–S(1) 136.6(3), C(25)–Pd(1)–S(1) 163.9(3), C(23)–Pd(1)–C(24) 38.1(5), C(23)–Pd(1)–C(25) 68.1(5), C(24)–Pd(1)–C(25) 37.5(5), Pd(1′)–N(1′) 2.128(9), Pd(1′)–S(1′) 2.356(3), Pd(1′)–C(23′) 2.169(10), Pd(1′)–C(24′) 2.171(10), Pd(1′)–C(25′) 2.159(11), N(1′)–Pd(1′)–S(1′) 85.0(3), N(1′)–Pd(1′)–C(23′) 167.2(4), N(1′)–Pd(1′)–C(24′) 133.3(4), N(1′)–Pd(1′)–C(25′) 99.9(4), C(23′)–Pd(1′)–S(1′) 105.2(3), C(24′)–Pd(1′)–S(1′) 141.0(3), C(25′)–Pd(1′)–S(1′) 164.8(3), C(23′)–Pd(1′)–C(24′) 38.4(4), C(25′)–Pd(1′)–C(23′) 68.3(4), C(25′)–Pd(1′)–C(24′) 38.7(4).

aziridine rings, which is (*S*) for complexes **9**, **10** and **11**. This arrangement avoids the steric interaction between the ferrocenylmethyl group on the nitrogen and the thioether moiety on the aziridine ring. It should also be noted that in all our cationic allylic Pd complexes the nitrogen atom generally forms a shorter bond [2.099(12)–2.150(6) Å] with palladium cation than other $sp^3$-hybridized nitrogen atoms.[24]

The X-ray structure analysis revealed that there were two independent conformations **9a** and **9a**′ in each asymmetric unit cell of the complex **9**, which had the same configuration. Additionally, the $\pi$-allyl moiety of the conformers **9a** and **9a**′ was found to be the *M*-type isomer (Fig. 1). That is, the central carbon atom of the allylic moiety was situated on the opposite side of the aziridine ring with respect to coordination plane of the palladium (II), minimizing the nonbonded repulsion between the central carbon atom of the allyl moiety and the methylene of the aziridine unit. This arrangement could rationalize the preference for the *M* orientation of the allylic ligand. The cyclopentyl group on sulfur and the aziridine unit was

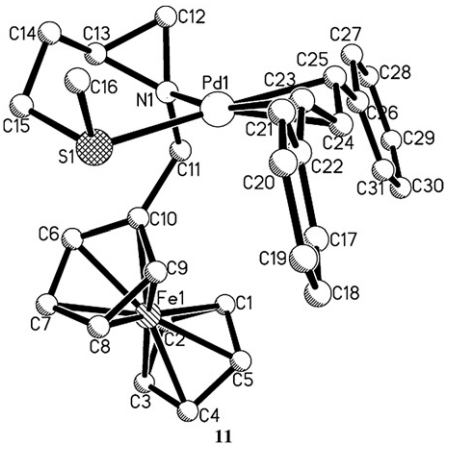


**Figure 4.** ORTEP drawing of the X-ray crystallographic structure and atom-numbering scheme of the cation **11**. Selected bond distances [Å] and angles [deg]: Pd(1)–N(1) 2.150(6), Pd(1)–S(1) 2.3709(19), Pd(1)–C(23) 2.190(6), Pd(1)–C(24) 2.152(7), Pd(1)–C(25) 2.181(7), C(22)–C(23) 1.479(10), C(23)–C(24) 1.386(10), N(1)–Pd(1)–S(1) 94.08(17), N(1)–Pd(1)–C(23) 162.4(2), N(1)–Pd(1)–C(24) 131.6(3), N(1)–Pd(1)–C(25) 96.6(2), C(23)–Pd(1)–S(1) 101.6(2), C(24)–Pd(1)–S(1) 131.9(2), C(25)–Pd(1)–S(1) 169.28(19), C(24)–Pd(1)–C(23) 37.2(3), C(25)–Pd(1)–C(23) 67.7(3), C(24)–Pd(1)–C(25) 38.3(3).

also located on the opposite side of the coordination plane of the palladium (II), avoiding the steric interaction between the cyclopentyl group and the methylene on the aziridine ring.

The values of the torsion angles Pd(1)–N(1)–C(13)–C(14) in **9a** and Pd(1′)–N(1′)–C(13′)–C(14′) in **9a**′ was 7.2(16)° and −1.5(15)°, respectively, indicating that the five-membered rings formed by the binding of the coordination atoms N and S to the palladium had envelope-like conformations, in which the sulfur atom deviated from the plane defined by the sets of atoms Pd(1)–N(1)–C(13)–C(14) in **9a**, and Pd(1′)–N(1′)–C(13′)–C(14′) in **9a**′, respectively.

As expected, the Pd–C bond lengths were different in cations **9a** and **9a**′, but a similar trend was found for the bond distances between the palladium (II) and the terminal carbon atoms of the allyl group [C(21) and C(23) in **9a** or C(21′) and C(23′) in **9a**′, respectively]. The bond between palladium and the terminal allylic carbon atom, which was trans to sulfur, was longer [2.216(14) Å in **9a** and 2.171(12) Å in **9a**′, respectively] than that trans to nitrogen (2.168(13) Å in **9a** and 2.132(11) Å in **9a**′, respectively). These structural data indicated that the sulfur atom was a better π-acceptor than the nitrogen atom. That is, the trans effect of the sulfur atom was higher than that of the nitrogen atom. Thus, if the active species in the reaction was the *M*-type, the nucleophile would attack the allylic terminus trans to sulfur, and as a result, the configuration of reaction products should be *S*, which was in agreement with our experimental result.

In accord with the complex **9**, the crystal structure analysis of **10** revealed that the allylic intermediate complex **10** also adopted the *M* configuration (Fig. 3). In addition, there also were two independent conformations **10a** and **10a**′ in each asymmetric unit cell of this complex, which had the same configuration.

The main difference between conformations **10a** and **10a**′ was that the different orientations (conformation) of ethyl group on the sulfur atom, due to the free rotation of carbon–carbon single bond, led to the significant distortion of the allylic unit for **10a** relative to **10a**′, as shown in **10**. In **10a**, a torsion angle C(14)–S(1)–C(15)–C(16) was −65.9(18)°, suggesting that C(16) and C(14) were gauched, while in **10a**′, a torsion angle C(14′)–S(1′)–C(15′)–C(16′) was 175.5(12)°, indicating that C(16′) and C(14′) were staggered, in which the methyl group on sulfur atom pointed toward the phenyl substituent on the carbon atom C(23′) of the allylic moiety. The C(23′)–Pd(1′)–S(1′) bond angle of 105.2(3)° in **10a**′ was larger than the C(23)–Pd(1)–S(1) bond angle of 100.7(4)° in **10a**, suggesting that the repulsion between the ethyl group on sulfur and the phenyl group on the carbon atom C(23′) in **10a**′ was stronger than the repulsion between the ethyl group on sulfur and the phenyl group on the carbon atom C(23) in **10a**. This strong nonbonded interaction in **10a**′ led to the phenyl group on carbon atom C(23′) to tilt up, and rotate anti-clockwise about C(23′)–C(22′) bond away from ethyl group relative to **10a**, as showed in Figure 3. Therefore, the conformation **10a** was more stable than **10a**′, and **10a** was preferential conformation. As expected, the Pd–C bond distances were significantly different in favored conformation **10a**. The bond distance between palladium and the terminal allylic carbon atom, which was *trans* to sulfur, was longer [Pd(1)–C(25)=2.197(14) Å] than that trans to nitrogen [Pd(1)–C(23)=2.136(13) Å], suggesting that the trans effect of the sulfur moiety was higher than that of nitrogen.

It was worth noting that in the contrast to situation in **10a**, the bond distance between palladium and the terminal allylic carbon atom in **10a**′, which was trans to sulfur, was shorter [Pd(1′)–C(25′)=2.159(11) (14) Å] than that trans to nitrogen [Pd(1′)–C(23′)=2.169(10) Å], suggesting that the trans effect of the nitrogen moiety was stronger than that of sulfur. This striking contrast between **10a** and **10a**′ was mainly caused by the local steric interaction between the substituents on the chiral ligand and the allylic moiety. For example, the C(23′)–Pd(1′)–S(1′) bond angle of 105.2(3)° in **10a**′ as well as the N(1)–Pd(1)–C(25) bond angle of 106.7(5)° in **10a** were larger than the N(1′)–Pd(1′)–C(25′) bond angle of 99.9(4)° in **10a**′, indicating that the weaker steric interaction between the ferrocenylmethyl group on nitrogen atom N(1′) and the phenyl group on the carbon atom C(25′) existed in **10a**′, which led to the Pd(1′)–C(25′) bond length to become shorter. These structural data suggested that the Pd–C bond lengths between palladium and the terminal allylic carbon atom were determined not only by electronic effects of two coordination atoms, but also by steric effects between the ligand and the allylic terminus. Hence, electronic effects as well as steric effects must be considered together. To the best of our knowledge, this is the first evidence that the conformational change of the same chiral ligand–Pd–π-allyl intermediate complex **10** results in the remarkable variations (opposite trends) of the bond distances between the palladium (II) and the terminal carbon atoms of the allyl unit, which has been characterized by X-ray diffraction.

Different to compounds **9** and **10**, only a single crystal of complex **11** was obtained. The X-ray crystal structure analysis confirmed that the allylic intermediate **11** also adopted the *M* configuration although the chiral ligand–Pd–π-allyl intermediate complex **11** formed six-membered ring chelate (Fig. 4). The six-membered chelating ring formed by the binding of the N and S atoms to the palladium was not on a plane; instead, it took a boatlike conformation. The obvious difference, compared with the allylic intermediate **9** and **10**, was that the methyl group on sulfur atom and the aziridine ring was located in *syn* side of the coordination plane of the palladium (II) in **11**.

The C(14) atom and the palladium deviated 3.289 Å from the main plane defined by the set of atoms N(1), C(13), C(15), and S(1). Because the methyl group on sulfur and the ferrocenylmethyl group on nitrogen were located on the different side of the chelate, the allylic intermediate **11** became sterically less congestion than the allylic intermediate **9** and **10**. As a result, this orientation minimized steric interaction between substituents on chiral ligand and phenyl groups of allylic moiety. For example, the N(1)–Pd(1)–C(25) bond angle of 96.6(2)° in **11** was much smaller than the corresponding N(1)–Pd(1)–C(21) bond angles of 102.3(5)° in **9a**, N(1)–Pd(1)–C(25) of 106.7(5)° in **10a**, respectively, indicating the minimal interaction between the ligand and the C(25) allylic terminus in **11**, which resulted in the shorter bond distance of the Pd(1)–C(25) in **11**. On the contrast, the C(23)–Pd(1)–S(1) bond angle of 101.6(2)° was

larger than the N(1)–Pd(1)–C(25) bond angle of 96.6(2)° in **11**, suggesting some interaction between the ligand and the C(23) allylic terminus. In accordance with the structural evidence for the allylic intermediate **9** and **10**, we also expected that the two palladium–terminal allyl carbon length of **11** would be different, with bond trans to sulfur longer than the bond trans to nitrogen. However, the actual bond distances of the Pd–C(23) and Pd–C(25) were 2.190(6), and 2.181(7) Å (almost equal with experimental error (0.009 Å, <0.5% difference)), respectively, indicating that the trans effect of the nitrogen moiety was slightly stronger than that of sulfur. If the active species in the reaction was the *M*-type, the attack of nucleophile would occur at the allylic carbon atom trans to nitrogen, giving the *R* configuration product, which was not in agreement with our experimental result (Table 1, entries 10 and 11). These results further suggested that the distances between palladium and terminal allyl carbon were determined not only by the electronic properties of two coordination atoms, but also by nonbonded interaction between the ligand and the allylic terminus.

### 2.5. NMR study of the palladium complexes of the ligands

Although the X-ray structures of **9**, **10**, and **11** showed that diastereomeric π-allyl complexes adopted only *M*-type for the π-allyl fragment, it was well precedented that palladium–allyl complexes isomerized, and gave two possible orientations (so-called *W*-type and *M*-type) for the π-allyl fragment with respect to the coordination plane in solution.[25] In addition, a different conclusion regarding trans effects of heterobidentate N,S-ligating atoms was drawn on the basis of the structural data of X-ray diffraction. In order to elucidate the solution structure of these complexes in $CD_2Cl_2$ (to reflect the reaction medium), some NMR and NOE experiments were carried out, in the hope of getting some insight into the favored formation of *M*- or *W*-type diastereomers in rotamers, and the ratio of two rotamers. NMR assignments for both stereoisomers were given in the Experimental Section.

$^1$H NMR studies of the complex **9** showed that the ratio of two stereoisomers **9A** and **9B** was about 1.8:1 at ambient temperature. Its configuration was assigned through a combination of COSY, $^{13}$C–$^1$H correlation (HSQC, HMBC) and NOE experiments. The $^1$H NMR showed only the *syn*,*syn* orientation of the allyl moiety, as confirmed by the coupling constants between the allylic protons H(23), H(22), and H(21) (labeled with H in **9A** and H′ in **9B**, respectively) of about 12 Hz and the presence of NOE between both terminal protons of the allylic group in the NOESY spectrum. According to the ORTEP diagram of **9a** (Fig. 1), the distance between the allylic termini H(21) and the aziridine H(12) was 3.50 Å. Therefore, a NOE between such hydrogen atoms should be observed. The NOESY spectrum showed the existence of such effect (Fig. 5). Though the NOE was weak, it was distinct in the 2D NOESY spectra with different exchange times such as 0.35, 0.55, 0.60 s. Thus, the major isomer of the complex **9** in solution was extrapolated to have the *M* configuration that was the same as the structure of the X-ray in solid state **9** (Fig. 1). In addition, a NOE cross-peak between the cyclopentyl group and the substituted Cp ring suggested that two groups were on the same side of the coordination plane, which was in accord with molecular modeling. At the same time, the cyclopentyl group and the substituted Cp ring had NOEs with the two phenyl groups of the allylic moiety in the major component, respectively, and no such effects could be identified in the minor component. The two terminus allyl protons [(H′(23) and H′(21), respectively)] had NOEs with protons of the substituted Cp ring in the minor isomer, suggesting that they were located on the same side of the chelate. These data further confirmed that the major intermediate was *M*-type configuretion in solution. NOE difference spectroscopy was also involved to evidence this conclusion by some key NOE enhancements. The signal of the allylic protons [(H(21) and H′(21), respectively)] was selectively irradiated for each of the two isomers. Irradiation of the signal at δ 5.56 ppm [H′(21) in the minor component] induced a significant enhancement of 15.7% at δ 4.52–4.21 ppm (protons of the substituted Cp ring). When the signal at δ 6.52 ppm [H(21) in the major component] was irradiated, a somewhat weaker enhancement of 0.43% was observed.

It was reported in the literature that there was a correlation between the $^{13}$C NMR chemical shifts of the carbons on the π-allyl termini and the relative positive charge (electrophilicity) of the carbon nucleus.[26] With such a correlation, the $^{13}$C NMR has been used to predict the reactivity of carbon termini of the palladium–allylic complexes. $^{13}$C–$^1$H NMR correlation pinpointed the terminal allyl carbon atoms: δ 87.2 (allylic carbon trans to S, C(21)) and δ 76.4 (allylic carbon trans to N, C(23)) for **9A** (Δδ=10.8), δ 85.5 (allylic carbon trans to S, C(21)) and δ 78.8 (allylic carbon trans to N, C(23)) for **9B** (Δδ=6.7). These data mean that the carbon atom C(21) on the π-allyl termini would be more sensitive than C(23) for nucleophilic attack, reflecting therefore the stronger trans effect of S relative to N, which corresponded to the X-ray results. Additionally, the enhanced downfield for C(21) of **9A** (δ 87.2) relative to C(21) of **9B** (δ 85.5), and the difference in chemical shift between C(21) and C(23) in **9A** (Δδ=10.8), compared with that for the identical carbons in **9B** (Δδ=6.7), allowed us to conclude that **9A** was more reactive than **9B**. Because nucleophilic attack at diastereomer **9A** was more favored, the product would be given in (*S*)-configuration. It was in agreement with our experimental results.

Compared to the complex **9**, the complex **10** possessed the same structural architectures and chiralities except for the different substituents on sulfur atoms. Therefore, the argument for complex **9** may also be applied to complex **10**. For **10**, a 1.5:1 ratio of the two isomers could be obtained from $^1$H NMR by the allylic protons. By a method similar to the assignment of the complex **9**, we could confirm only *syn*,*syn* arrangement of the allyl unit (Fig. 6). Through a combination of $^1$H NMR, COSY, $^1$H–$^{13}$C NMR, and NOE experiments (Fig. 6), the major isomer was assigned as *M*-type (Fig. 1), which was just the same as the structure of the X-ray (Fig. 2). Terminal $^{13}$C allyl chemical shifts are δ 75.7 (allyl carbon trans to N, C(23)) and δ 88.0 (allyl carbon trans to S, C(25)) for **10A** (Δδ=12.3); and δ 78.2 (allyl carbon trans to N, C(23)) and δ 86.1 (allyl carbon trans to S, C(25)) for **10B** (Δδ=8.1). This information suggested that **10A** was more reactive than **10B**, and the trans effect of S was stronger than that of N.

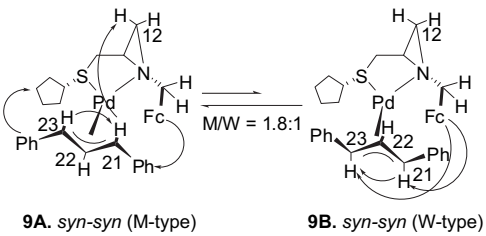


**9A.** *syn-syn* (M-type) **9B.** *syn-syn* (W-type)

**Figure 5.** Relevant NOE contacts from NOESY experiment of complex **9**.

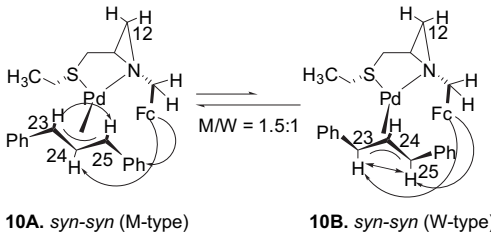


**10A.** *syn-syn* (M-type) **10B.** *syn-syn* (W-type)

**Figure 6.** Relevant NOE contacts from NOESY experiment of complex **10**.

It should also be noted that the enantiomeric excess (Table 1, entries 4 and 8, 87% ee for **3a**, 83% ee for **3b**, respectively; Table 2, entries 7 and 2, 89% ee for **3a**, and 91% ee for **3b**, respectively) of the reaction product did not reflect the isomeric distribution (the de of the active species is 28% for **3a**, 20% for **3b**, respectively) of the π-allyl complexes. The high enantioselectivities observed would be rationalized by the NMR spectroscopic data. For the π-allyl complexes **9** and **10**, the major isomers **9A** and **10A** were more active than minor isomers **9B** and **10B**, and furthermore, the allyl termini trans to sulfur atom were more sensitive than that trans to nitrogen atom for nucleophilic attack.

At the same time, the X-ray structures combined with the NMR data suggested that the high enantioselectivities observed were also the results of a Curtin–Hammett condition[27] in which the attack of nucleophile at the allylic carbon atom trans to sulfur would occur faster in the major isomers **A** than in the minor isomers **B**, when palladium–allyl complexes isomerized fast in solution. The different reactivity of the two isomers could also be explained by steric interactions developed during the transition state (Scheme 4).[7e] In the major isomer **A**, there were steric interactions between the ferrocenyl substituent on the ligand and the proximal phenyl substituent on the π-allyl moiety. Upon nucleophilic addition, the steric strain was released to form the palladium–olefin complex **12**. In the minor diastereomeric complex **B**, there was no steric strain that was present in **A**. Upon nucleophilic addition to the palladium–olefin complex **B**, unfavorable steric interactions would be developed, affording the palladium–olefin complex **13**. Minimization of this interaction was therefore the reason that nucleophilic addition occurred faster in the major diastereomeric π-allyl complex **A** than that of **B**. These results suggested that the bulky ferrocenyl substituent at the N atom showed a high enantiocontrol, and steric effect of the ferrocenyl group played an important role in the allylic substitution reactions.

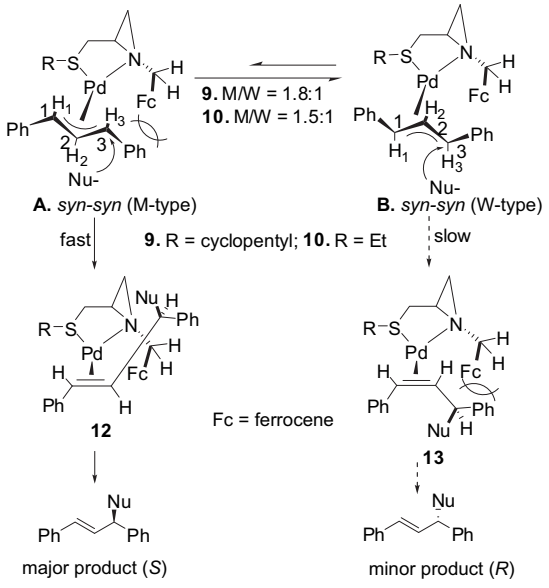


**Scheme 4.** Selectivity of the dimethyl malonate attack on the terminal allylic carbon atoms of complexes **9** and **10**.

For complex **11**, the $^1$H NMR spectrum at room temperature showed that there was a mixture of two conformers in a ratio of 2.5:1, and their configuration were assigned by a combination of COSY, $^{13}$C–$^1$H correlation, HMBC, and NOE experiments as detailed above for complex **9** and **10**. The $^1$H NMR and NOE studies manifested only the *syn–syn* arrangement of the allylic unit. Consistent with **9** and **10**, the results revealed that the *M*-type configuration of allylic moiety (*syn–syn*) was the major isomer. According to the ORTEP diagram of **11** (Fig. 4), the distance between the allylic termini H (25) and the aziridine H(12) was 3.33 Å. A NOE between such hydrogen atoms suggested the existence of such effect (Fig. 7). However, in the *W*-type configuration, no such effect occurred because H(25) and H(12) point in the opposite direction. In addition, the two phenyl groups had NOEs with the substituted Cp ring in the major component and no such effects could be found in the minor component. NOEs between the two terminus allyl protons (H′(23) and H′(25), respectively) and protons of the substituted Cp ring also suggested that the minor isomer should be the *W*-type configuration. Such assignment was also confirmed by NOE difference spectroscopy. Irradiation of the signal at $\delta$ 6.70 ppm H(24) induced an enhancement at $\delta$ 4.41 ppm (substituted Cp ring). When the signal at $\delta$ 6.52 ppm H(24′) was irradiated, no such enhancement was induced. This suggested that the ferrocenylmethyl group and the central allyic proton were on the same side of the chelate in the major conformer, corresponding to the X-ray results. Terminal $^{13}$C allyl chemical shifts in the major isomer **11A** were $\delta$=86.1 (allyl carbon trans to S, C(25)) and 77.0 (trans to N, C(23)), respectively, with ($\Delta\delta$=9.1); corresponding shifts in the minor isomer **11B** were $\delta$=84.0 (allyl carbon trans to S, C(25)) and 79.0 (trans to N, C(23)), respectively, with ($\Delta\delta$=5.0). These results reflected the stronger trans effect of the sulfur ligand than that of the nitrogen ligand, and the major isomer **11A** had a higher reactivity. Then one would predict that the product from **11A** was obtained by attacking the carbon atom with $\delta$ 86.1, thus giving a (*S*)-configuration product with moderate enantioselectivity (Table 1, entry 11, 75% ee), which was in accord with the experimental result.

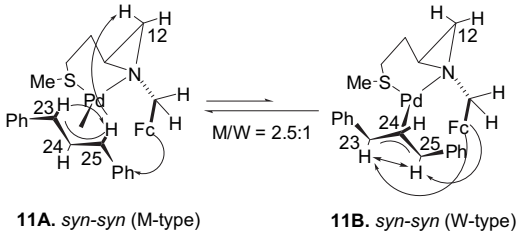


**Figure 7.** Relevant NOE contacts from NOESY experiment of complex **11**.

## 3. Conclusion

In summary, we have prepared a new class of chiral of sulfide ligands **3a–c**, **6** containing both the ferrocenyl skeleton and the aziridine unit from (*R*)-cysteine or L-(+)-methionine. The chiral ligands **3a–c** are effective catalysts for palladium-catalyzed allylic substitution reactions with enantioselectivity of up to 91% ee. The effect of different bases used to yield the dimethyl malonate anion was also evaluated in this reaction. In the absence of KOAc, the allylic alkylation proceeded well under our conditions, suggesting that BSA acted only as a silyating reagent of dimethyl malonate to generate a ketene silyl acetal, did not work as a base. The comparisons of the crystal structures revealed that that the Pd–C bond lengths between palladium and the terminal allylic carbon atom were determined not only by electronic effects of two coordination atoms, but also by steric effects between the ligand and the allylic terminus. What differentiates this study from other published ligand system is that a different conclusion may be drawn when trans effects of heterobidentate coordination atoms are determined only based on the structural data of X-ray diffraction. Therefore, both structural data in the solid state and the structural information in the solution must be considered together. NMR spectroscopic data may complement X-ray crystallographic data. The sense and level of asymmetric induction of heterobidentate sulfide-tertiary amine ($sp^3$) ligands were first rationalized based on X-ray

crystallographic data, and NMR spectroscopic data for relevant intermediate palladium–allylic complexes. Our results demonstrated that the sulfur atom was a better π-allyl acceptor than the nitrogen atom for heterobidentate sulfide-tertiary amine ($sp^3$) ligands, and the steric as well electronic properties of the intermediate palladium–allylic complexes were crucial for the enantioselectivity. Efforts to extend the application of these ligands to other enantioselective metal-catalyzed reactions are also in progress.

## 4. Experimental

### 4.1. General

Unless otherwise noted, all reactions were carried out under argon or nitrogen using standard Schlenk and vacuum line techniques. $[Pd(\eta^3\text{-PhCHCHCHPh})Cl]_2$ was prepared by using literature procedures.[28] THF was distilled from sodium/benzophenone, dichloromethane, acetonitrile, and toluene were freshly distilled over calcium hydride prior to use. Other reagents were obtained from commercial sources and used as received without further purification. Melting points were determined using YRT-3 melting point apparatus and are uncorrected. Elemental analyses were determined with a Carlo Erba 1160 elemental analyzer. Optical rotations were measured with Perkin Elmer, model 341 Polarimeter at 20 °C in $CHCl_3$. The enantiomeric purity was determined by HPLC using a chiral column with hexane/propan-2-ol (ratio as indicated) as the eluent. The chromatographic system consisted of a JASCO model PU-1580 intelligent HPLC pump and a JASCO model UV-1575 intelligent UV–vis detector (254 nm). The injection loop had a 20 μL capacity. The column used was a Chiralcel OD (250×4.6 mm) from Daicel Chemical Ind., Ltd (Japan). The column was operated at ambient temperature. NMR spectra ($^1H$ and $^{13}C$) were performed on a Bruker DPX 400 (400 MHz) spectrometer using solutions in $CDCl_3$ or $CD_2Cl_2$ (referenced internally to $Me_4Si$); *J* values are given in Hz. For 1D NOE difference experiments a 10 s overall recycle delay with 8 s irradiation time and an in-house written pulse sequence were used. A long train of 90 degree Gaussian pulses provided selective saturation of the selected signals. IR spectra were determined on a Thermo Nicolet IR 200 spectrophotometer. TLC was performed on dry silica gel plates developed with hexane/ethyl acetate. Mass spectra were obtained using a Bruker esquire-3000 instrument with an electrospray ionization source (ESIMS). All the ESIMS spectra were performed using MeOH as the solvent. Methanol was dried with $Mg(OCH_3)_2$.

### 4.2. Synthesis of $[Pd(\eta^3\text{-1,3-diphenylallyl})(\mathbf{3a})]^+SbF_6^-$ (9)

To a solution of ligand **3a** (107 mg, 0.31 mmol) in MeOH/$CH_2Cl_2$ (v/v 1:1 ml) was added 1,3-diphenylallyl-palladium chloride dimer (104 mg, 0.31 mmol). After 30 min, $AgSbF_6$ (106 mg, 0.31 mmol) was added, and stirring continued in the absence of light. After 2 h, the reaction mixture was filtered through Celite, and washed with MeOH/$CH_2Cl_2$ (v/v 1:1). The resulting solid was recrystallized from dichloromethane/hexane, and gave 168 mg (61%) of complex **9**. Further recrystallizations from dichloromethane/hexane afforded red crystals suitable for X-ray crystallography, mp 223–226 °C (dec); $[\alpha]_D^{20}$ −17.2 (*c* 1.00, $CH_2Cl_2$). $^1H$ NMR (400 MHz, $CD_2Cl_2$) two isomers (1.8/1), Major **9A**: δ=7.90–7.88 (m, 2H, Ar), 7.64–7.55 (m, 8H, Ar), 6.82 (t, $^2J$=12.1 Hz, 1H, central allyl H), 5.56 (d, $^2J$=12.7 Hz, 1H, allylic H trans to S), 5.19 (d, $^2J$=11.6 Hz, 1H, allylic H trans to N), 4.20–3.96 (m, 9H, Fc), 3.11–3.09 (m, 1H, SCH*H*), 2.70 (d, $^1J$=12.9 Hz, 1H, FcCH*H*), 2.67–2.64 (m, 1H, SC*H*H), 2.53–2.49 (m, 1H, NCH*H*), 2.38–2.34 (m, 1H, NC*H*H), 2.36–2.93 (m, 1H, NC*H*), 2.04 (d, $^1J$=13.1 Hz, 1H, FcC*H*H), 1.94–1.86 (m, 1H, cyclopentyl), 1.72–1.68 (m, 1H, cyclopentyl), 1.60–0.89 (m, 6H, cyclopentyl), 0.09–0.06 (m, 1H, cyclopentyl); minor **9B**: δ=7.79–7.77 (m, 2H, Ar), 7.35–7.31 (m, 8H, Ar), 6.61 (t, $^2J$=11.7, 1H, central allyl H), 5.03 (d, $^2J$=11.6 Hz, 1H, allylic H trans to S), 4.82 (d, $^2J$=11.7 Hz, 1H, allylic H trans to S), 4.52–4.15 (m, 9H, Fc), 3.51 (d, $^1J$=13.1 Hz, 1H, FcCH*H*), 3.14–3.13 (m, 1H, SCH*H*), 2.53–2.49 (m, 1H, SC*H*H), 2.38–2.34 (m, 3H, FcC*H*H+NC*H*+cyclopentyl), 1.94–1.86 (m, 2H, NC$H_2$), 1.60–0.89 (m, 8H, cyclopentyl). $^{13}C$ NMR (100 MHz, $CD_2Cl_2$), Major **9A**: δ=105.9 (central allyl), 87.2 (allyl trans to S), 76.4 (allyl trans to N); minor **9B**: δ=108.7 (central allyl), 85.5 (allyl trans to S), 78.8 (allyl trans to N). MS: *m*/*z* (ESI) 654 ($M^+$−$SbF_6$). HRMS-ESI *m*/*z* calcd for $C_{34}H_{38}FeNPdS$ 654.1109, found 654.1108. Anal. Calcd for $C_{34}H_{38}F_6FeNPdSSb$: C, 45.84; H, 4.30; N, 1.57; S, 3.60. Found: C, 46.11; H, 4.65; N, 1.51; S, 3.40.

### 4.3. Synthesis of $[Pd(\eta^3\text{-1,3-diphenylallyl})(\mathbf{3b})]^+SbF_6^-$ (10)

The complex **10** was synthesized in a fashion similar to that described for **9**; a red crystal was obtained in 67% yield, mp 208–211 °C (dec). $[\alpha]_D^{20}$ +154.8 (*c* 1.00, $CH_2Cl_2$). $^1H$ NMR (400 MHz, $CD_2Cl_2$) two isomers (1.5/1), Major **10A**: δ=7.90–7.88 (m, 2H, Ar), 7.61–7.55 (m, 8H, Ar), 6.76 (t, $^2J$=12.0 Hz, 1H, central allyl H), 5.58 (d, $^2J$=12.5 Hz, 1H, allylic H trans to S), 5.06 (d, $^2J$=11.5, 1H, allylic H trans to N), 4.40–3.96 (m, 9H, Fc), 3.18–3.13 (m, 1H, SCH*H*), 2.77 (d, $^1J$=13.0, 1H, FcCH*H*), 2.73–2.64 (m, 1H, SC*H*H), 2.49–2.46 (m, 1H, NC*H*), 2.56–2.34 (m, 2H, NC$H_2$), 2.12 (d, $^1J$=13.0 Hz, 1H, FcC*H*H), 1.84–1.82 (m, 1H, $CH_3$CH*H*), 1.58–1.53 (m, 1H, $CH_3$C*H*H), 0.46 (t, $^2J$=12.9 Hz, 3H, C$H_3$); minor **10B**: δ=7.80–7.78 (m, 2H, Ar), 7.37–7.33 (m, 8H, Ar), 6.63 (t, $^2J$=11.7 Hz, 1H, central allyl H), 5.04 (d, $^2J$=11.5 Hz, 1H, allylic H trans to S), 4.87 (d, $^2J$=11.7 Hz, 1H, allylic H trans to N), 4.40–3.96 (m, 9H, Fc), 3.49 (d, $^1J$=13.2 Hz, 1H, FcCH*H*), 3.13–3.08 (m, 1H, SCH*H*), 2.73–2.64 (m, 1H, SC*H*H), 2.49–2.47 (m, 1H, FcC*H*H), 2.30–2.26 (m, 1H, NC*H*), 2.06–1.93 (m, 3H, NC*H*H+SC*H*H), 1.82–1.77 (m, 1H, NC*H*H), 0.93 (t, $^2J$=12.9 Hz, 3H, C$H_3$). $^{13}C$ NMR (100 MHz, $CD_2Cl_2$), Major **10A**: δ=107.1 (central allyl C), 88.0 (allyl C trans to S), 75.7 (allyl C trans to N); minor **10B**: δ=108.8 (central allyl C), 86.1 (allyl C trans to S), 78.2 (allyl C trans to N). MS: *m*/*z* (ESI) 614 ($M^+$−$SbF_6$). HRMS-ESI *m*/*z* calcd for $C_{31}H_{34}FeNPdS$ 614.0796, found 614.0791. Anal. Calcd for $C_{31}H_{34}F_6FeNPdSSb$: C, 43.77; H, 4.03; N, 1.65; S, 3.77. Found: C, 44.03; H, 4.11; N, 1.58; S, 3.75.

### 4.4. Synthesis of $[Pd(\eta^3\text{-1,3-diphenylallyl})(\mathbf{6})]^+SbF_6^-$ (11)

This complex was synthesized in a fashion similar to that described for **9**; a red crystal was obtained in 88% yield, mp 207–210 °C (dec). $[\alpha]_D^{20}$ +161.8 (*c* 1.00, $CH_2Cl_2$). $^1H$ NMR (400 MHz, $CD_2Cl_2$) two isomers (2.5/1), Major **11A**: δ=7.87–7.84 (m, 2H, Ar), 7.54–7.49 (m, 4H, Ar), 7.40–7.33 (m, 4H, Ar), 6.70 (t, $^2J$=11.8 Hz, 1H, central allyl H), 5.25 (d, $^2J$=12.4 Hz, 1H, allylic H trans to S), 4.64 (d, $^2J$=11.4, 1H, allylic H trans to N), 4.41–3.95 (m, 9H, Fc), 2.58–2.55 (m, 1H, 14-H), 2.40–2.36 (m, 1H, FcCH*H*), 2.22–2.21 (m, 1H, SCH*H*), 2.22–2.20 (m, 1H, NCH*H*), 1.92–1.89 (m, 1H, NC*H*H), 1.89–1.81 (m, 2H, NC*H*+SC*H*H), 1.78 (d, $^1J$=12.9, 1H, FcC*H*H), 1.44 (s, 3H, C$H_3$), 1.38–1.11 (m, 1H, 14–H); minor **11B**: δ=7.68–7.66 (m, 2H, Ar), 7.60–7.57 (m, 8H, Ar), 6.52 (t, *J*=11.8 Hz, 1H, central allyl H), 4.96 (d, $^2J$=11.6 Hz, 1H, allylic H trans to S), 4.86 (d, $^2J$=11.9 Hz, 1H, allylic H trans to N), 4.41–3.95 (m, 9H, Fc), 3.78 (d, $^2J$=12.8 Hz, 1H, FcCH*H*), 2.51–2.45 (m, 1H, FcC*H*H), 2.33–2.28 (m, 1H, 14-H), 2.12–2.05 (m, 1H, SCH*H*), 1.93–1.91 (m, 1H, SC*H*H), 1.87–1.82 (m, 1H, NC*H*), 1.36–1.29 (m, 1H, NCH*H*), 1.18–1.15 (s, 3H, C$H_3$), 1.12–1.10 (m, 1H, NC*H*H), 0.92–0.83 (m, 1H, 14-H). $^{13}C$ NMR (100 MHz, $CD_2Cl_2$), Major **11A**: δ=108.2 (central allyl), 86.1 (allyl trans to S), 77.0 (allyl trans to N); minor **11B**: δ=106.3 (central allyl), 84.0 (allyl trans to S), 79.0 (allyl trans to N). MS: *m*/*z* (ESI) 614 ($M^+$−$SbF_6$). HRMS-ESI *m*/*z* calcd for $C_{31}H_{34}FeNPdS$ 614.0796, found 614.0799. Anal. Calcd for $C_{31}H_{34}F_6FeNPdSSb$: C, 43.77; H, 4.03; N, 1.65; S, 3.77. Found: C, 44.02; H, 4.08; N, 1.59; S, 3.75.

### 4.5. General procedure for palladium-catalyzed allylic alkylation with dimethyl sodiumalonate as nucleophi1e

A THF solution of $[Pd(\eta^3\text{-}C_3H_5)Cl]_2$ (3.7 mg, 0.01 mmol) and the ligand (0.01 mmol) was stirred for 1 h at room tempreture under nitrogen atmosphere, and then 1,3-diphenyl-2-propenyl acetate (106 mg, 0.4 mmol) was added. The mixture was stirred for 15 min, and a solution of sodium dimethyl malonate, prepared from dimethyl malonate (132 mg, 1.0 mmol), and NaH (24 mg, 1.0 mmol) in THF (3 mL) was added at 0 °C. The mixture was stirred at 0 °C for the time given as in Table 1. The reaction was quenched with satd $NH_4Cl$ (aq), and extracted with $CH_2Cl_2$ (3×10 mL). The combined organic layers were dried over $Na_2SO_4$. The solvent was evaporated and the crude product was purified by silica gel with hexane/EtOAc (5:1). The ee was determined by HPLC (chiracel OD, 2-propanol/hexane=1:100, flow rate 0.5 mL/min $\lambda$=254 nm). The absolute configuration of the product was assigned by comparing the sign of its specific rotation with literature data.[20]

### 4.6. General procedure for palladium-catalyzed allylic alkylation using BSA procedure

To $[Pd(\eta^3\text{-}C_3H_5)Cl]_2$ (3.7 mg, 0.01 mmol) was added a solution of the ligand (0.01 mmol) in anhydrous THF (1 mL). The resultant solution was stirred for 1 h at room temperature under nitrogen atmosphere, and then 1,3-diphenyl-2-propenyl acetate (106 mg, 0.4 mmol) in anhydrous THF (1 mL) was added. The mixture was stirred for 15 min. Where upon, dimethyl malonate (158 mg, 0.14 mL, 1.2 mmol) and BSA (240 mg, 0.3 mL, 1.2 mmol) were added sequentially. The solution was stirred at room temperature under argon for the time as noted in Table 2. The reaction was quenched with satd $NH_4Cl$ (aq), and extracted with $CH_2Cl_2$ (3×10 mL). The combined organic layers were dried over $Na_2SO_4$. The solvent was evaporated and the crude product was purified by silica gel with hexane/EtOAc (5:1). The ee was determined by HPLC (chiracel OD, 2-propanol/hexane=1:100, flow rate 0.5 mL/min, $\lambda$=254 nm).

### 4.7. X-ray crystallographic study

A prismatic crystal of **9** (0.20×0.18×0.17), **10** (0.20×0.18×0.18 mm), and **11** (0.18×0.16×0.14 mm) were selected and mounted on a glass fiber, respectively. Crystallographic data for **9**, **10**, and **11** were measured on a Rigaku RAXIS-IV imaging plate area detector, respectively. The data were collected at 291(2) K using graphite-monochromated Mo Kα ($\lambda$=0.71073 Å), $1.16° < \theta < 25.50°$ for **9**, $1.14° < \theta < 25.50°$ for **10**, and $1.84° < \theta < 26.00°$ for **11**, respectively. The structures were solved by a direct method, and expanded by using Fourier techniques. The non-hydrogen atoms were refined anisotropically. Hydrogen atoms were included but not refined. All calculations were performed using the teXsan crystallographic software package. Crystal data for **9**: triclinic $P_1$, $a$=10.438(2) Å, $\alpha$=75.80(3)°, $b$=10.929(2) Å, $\beta$=88.91(3)°, $c$=18.172(4) Å, $\gamma$=62.66(3)°, $V$=1774.7(6) Å$^3$; formula unit $C_{34}H_{38}F_6FeNPdSSb$ with $Z$=2, $D_{calcd}$=1.667 g cm$^{-3}$, $F$(000)=884, $\mu$(Mo Kα)=1.774 mm$^{-1}$. Full-matrix least-squares refinement on $F^2$ based on 6142 independent reflections ($R_{int}$=0.0000) converged with 684 parameters. Final $R$ indices [$I>2\sigma(I)$]: $R_1$=0.532, $wR_2$=0.1313; $R$ indices (all data): $R_1$=0.0579, $wR_2$=0.1361; $GoF$=1.037. Crystal data for **10**: triclinic $P_1$, $a$=9.915(2) Å, $\alpha$=84.61(3)°, $b$=10.292(2) Å, $\beta$=74.79(3)°, $c$=18.506(4) Å, $\gamma$=63.53(3)°, $V$=1630.8(6) Å$^3$; formula unit $C_{31}H_{34}F_6FeNPdSSb$ with $Z$=2, $D_{calcd}$=1.732 g cm$^{-3}$, $F$(000)=840, $\mu$(Mo Kα)=1.926 mm$^{-1}$. Full-matrix least-squares refinement on $F^2$ based on 5686 independent reflections ($R_{int}$=0.0000) converged with 684 parameters. Final $R$ indices [$I>2\sigma(I)$]: $R_1$=0.478, $wR_2$=0.1291; $R$ indices (all data): $R_1$=0.0498, $wR_2$=0.1315; $GoF$=1.033. Crystal data for **11**: orthorhombic, $P2_12_12_1$, $a$=13.280(3) Å, $\alpha$=90°, $b$=14.310(3) Å, $\beta$=90°, $c$=17.390(4) Å, $\gamma$=90°, $V$=3304.7(12) Å$^3$; formula unit $C_{31}H_{34}F_6FeNPdSSb$ with $Z$=4, $D_{calcd}$=1.710 g cm$^{-3}$, $F$(000)=1680, $\mu$(Mo Kα)=1.901 mm$^{-1}$. Full-matrix least-squares refinement on $F^2$ based on 6152 independent reflections ($R_{int}$=0.0340) converged with 336 parameters. Final $R$ indices [$I>2\sigma(I)$]: $R_1$=0.0497, $wR_2$=0.1349; $R$ indices (all data): $R_1$=0.0546, $wR_2$=0.1413; $GoF$=1.088. CCDC-718824 (**9**), -718822 (**10**), and -718823 (**11**) contain the supplementary crystallographic data for this paper. These data can be obtained free of charge from The Cambridge Crystallographic Data Centre at www.ccdc.cam.ac.uk/data_request/cif.


## Acknowledgements

We are grateful to the Innovation Fund for Outstanding Scholar of Henan Province (074200510005), the National Natural Sciences Foundation of China (NNSFC: 20672102), and Henan Outstanding Youth Program (084100410001).


## Supplementary data

Supplementary data associated with this article can be found in the online version, at doi: 10.1016/j.tet.2009.08.037.

## References and notes


1. For reviews and highlights on applications, see (a) Fan, Q.-H.; Li, Y.-M.; Chan, A. S. C. *Chem. Rev.* **2002**, *102*, 3385–3466; (b) Trost, B. M.; Crawley, M. L. *Chem. Rev.* **2003**, *103*, 2921–2943; (c) Trost, B. M. *J. Org. Chem.* **2004**, *69*, 5813–5837; (d) Tunge, J. A.; Burger, E. C. *Eur. J. Org. Chem.* **2005**, *9*, 1715–1726; (e) You, S. L.; Dai, L. X. *Angew. Chem., Int. Ed.* **2006**, *45*, 5246–5248; (f) Graening, T.; Schmalz, H. G. *Angew. Chem., Int. Ed.* **2003**, *42*, 2580–2854; (g) Braun, M.; Meier, T. *Angew. Chem., Int. Ed.* **2006**, *45*, 6952–6955.
2. Trost, B. M.; Strege, P. E. *J. Am. Chem. Soc.* **1977**, *99*, 1649–1651.
3. For recent examples: (a) Glos, M.; Reiser, O. *Org. Lett.* **2000**, *2*, 2045–2048; (b) Chelucci, G.; Pinna, G. A.; Saba, A.; Sanna, G. *J. Mol. Catal. A: Chem* **2000**, *159*, 423–427; (c) Bolm, C.; Simic, O.; Martin, M. *Synlett* **2001**, 1878–1880; (d) Pericas, M. A.; Puigjaner, C.; Riera, A.; Vidal-Ferran, A.; Gomez, M.; Jimenez, F.; Muller, G.; Rocamora, M. *Chem.—Eur. J.* **2002**, *8*, 4164–4178; (e) Ait-Haddou, H.; Hoarau, O.; Cramailere, D.; Pezet, F.; Daran, J.-C.; Balavoine; Gilbert, G. A. *Chem.—Eur. J.* **2004**, *10*, 699–707; (f) Bayardon, J.; Sinou, D.; Guala, M.; Desimoni, G. *Tetrahedron: Asymmetry* **2004**, *15*, 3195–3200; (g) Bayardon, J.; Sinou, D. *J. Org. Chem.* **2004**, *69*, 3121–3128; (h) Vasse, J.-L.; Stranne, R.; Zalubovskis, R.; Gayet, C.; Moberg, C. *J. Org. Chem.* **2003**, *68*, 3258–3270; (i) Perez, S.; Lopez, C.; Bosque, R.; Solans, X.; Font-Bardia, M.; Roig, A.; Molins, E.; van Leeuwen, P. W. N. M.; van Strijdonck, G. P. F.; Freixa, Z. *Organometallics* **2008**, *27*, 4288–4299; (j) Zalubovskis, R.; Bouet, A.; Fjellander, E.; Constant, S.; Linder, D.; Fischer, A.; Lacour, J.; Privalov, T.; Moberg, C. *J. Am. Chem. Soc.* **2008**, *130*, 1845–1855.
4. For recent examples: (a) Dieguez, M.; Pamies, O.; Claver, C. *J. Org. Chem.* **2005**, *70*, 3363–3368; (b) Malaise, G.; Ramdeehul, S.; Osborn, J. A.; Barloy, L.; Kyritsakas, N.; Graff, R. *Eur. J. Inorg. Chem.* **2004**, 3987–4001; (c) Xie, J.-H.; Duan, H.-F.; Fan, B.-M.; Cheng, X.; Wang, L.-X.; Zhou, Q.-L. *Adv. Synth. Catal.* **2004**, *346*, 625–632; (d) Dieguez, M.; Pamies, O.; Claver, C. *Adv. Synth. Catal.* **2005**, *347*, 1257–1266; (e) Raghunath, M.; Zhang, X. *Tetrahedron Lett.* **2005**, *46*, 8213–8216; (f) Chen, X.; Guo, R.; Li, Y.; Chen, G.; Yeung, C.-H.; Chan, A. S. C. *Tetrahedron: Asymmetry* **2004**, *15*, 213–217; (g) Zhao, D.; Sun, J.; Ding, K. *Chem.—Eur. J.* **2004**, *10*, 5952–5963; (h) Raluy, E.; Claver, C.; Pamies, O.; Dieguez, M. *Org. Lett.* **2007**, *9*, 49–52; (i) Favier, I.; Gomez, M.; Muller, G.; Axet, M. R.; Castillon, S.; Claver, C.; Jansat, S.; Chaudret, B.; Philippot, K. *Adv. Synth. Catal.* **2007**, *349*, 2459–2469; (j) Liu, D.; Xie, F.; Zhang, W. *J. Org. Chem.* **2007**, *72*, 6992–6997; (k) Raluy, E.; Dieguez, M.; Pamies, O. *J. Org. Chem.* **2007**, *72*, 2842–2850; (l) Sharma, R. K.; Nethaji, M.; Samuelson, A. G. *Tetrahedron: Asymmetry* **2008**, *19*, 655–663.
5. Selected examples: (a) Fukuzumi, T.; Shibata, N.; Sugiura, M.; Yasui, H.; Nakamura, S.; Toru, T. *Angew. Chem., Int. Ed.* **2006**, *45*, 4973–4977; (b) Bower, J. F.; Jumnah, R.; Williams, A. C.; Williams, J. M. J. *J. Chem. Soc., Perkin Trans. 1* **1997**, 1411–1420; (c) Togni, A.; Burckhardt, U.; Gramlich, V.; Pregosin, P. S.; Salzmann, R. *J. Am. Chem. Soc.* **1996**, *118*, 1031–1037; (d) Froelander, A.; Lutsenko, S.; Privalov, T.; Moberg, C. *J. Org. Chem.* **2005**, *70*, 9882–9891; (e) Hou, D.-R.; Reibenspies, J. H.; Burgess, K. *J. Org. Chem.* **2001**, *66*, 206–215; (f) Danjo, H.; Higuchi, M.; Yada, M.; Imamoto, T. *Tetrahedron Lett.* **2004**, *45*, 603–606; (g) Sun, X.-M.; Koizumi, M.; Manabe, K.; Kobayashi, S. *Adv. Synth. Catal.* **2005**, *347*, 1893–1898; (h) You, S.-L.; Hou, X.-L.; Dai, L.-X.; Yu, Y.-H.; Xia, W. *J. Org. Chem.* **2002**, *67*, 4684–4695; (i) Manoury, E.; Fossey, J. S.; Aiet-Haddou, H.; Daran, J.-C.; Balavoine, G. G. A. *Organometallics* **2000**, *19*, 3736–3739; (j) Deng, W.-P.; You, S.-L.; Hou, X.-L.; Dai, L.-X.; Yu, Y.-H.; Xia, W.; Sun, J. *J. Am. Chem. Soc.* **2001**, *123*, 6508–6519; (k) You, S.-L.; Zhu, X.-Z.; Luo, Y.-M.; Hou, X.-L.; Dai, L.-X. *J. Am. Chem. Soc.* **2001**, *123*, 7471–7472; (l) Mata, Y.; Dieguez, M.; Pamies, O.; Claver, C. *Adv. Synth. Catal.* **2005**, *347*, 1943–1947; (m) Selvakumar, K.; Valentini, M.; Pregosin, P. S.; Albinati, A.; Eisentraeger, F. *Organometallics* **2000**, *19*, 1299–

1307; (n) Widhalm, M.; Nettekoven, U.; Kalchhauser, H.; Mereiter, K.; Calhorda, M. J.; Felix, V. *Organometallics* **2002**, *21*, 315–325; (o) Pamies, O.; Dieguez, M.; Claver, C. *J. Am. Chem. Soc.* **2005**, *127*, 3646–3647; (p) Mino, T.; Saito, A.; Tanaka, Y.; Hasegawa, S.; Sato, Y.; Sakamoto, M.; Fujita, T. *J. Org. Chem.* **2005**, *70*, 1937–1940; (q) Mino, T.; Tanaka, Y.; Hattori, Y.; Yabusaki, T.; Saotome, H.; Sakamoto, M.; Fujita, T. *J. Org. Chem.* **2006**, *71*, 7346–7353; (r) Jiang, B.; Lei, Y.; Zhao, X.-L. *J. Org. Chem.* **2008**, *73*, 7833–7836; (s) Popa, D.; Puigjaner, C.; Gomez, M.; Benet-Buchholz, J.; Vidal-Ferran, A.; Pericas, M. A. *Adv. Synth. Catal.* **2007**, *349*, 2265–2278; (t) Fukuzawa, S.; Oki, H.; Hosaka, M.; Sugasawa, J.; Kikuchi, S. *Org. Lett.* **2007**, *9*, 5557–5560.

6. Selected examples: (a) Frost, C. G.; Williams, J. M. J. *Tetrahedron: Asymmetry* **1993**, *4*, 1785–1788; (b) Chesney, A.; Bryce, M. R.; Chubb, R. W. J.; Batsanov, A. S.; Howard, J. A. K. *Tetrahedron: Asymmetry* **1997**, *8*, 2337–2346; (c) Allen, J. V.; Coote, S. J.; Dawson, G. J.; Frost, C. G.; Martin, C. J.; Williams, J. M. J. *J. Chem. Soc., Perkin Trans. 1* **1994**, 2065–2072; (d) Bolm, C.; Kaufmann, D.; Zehnder, M.; Neuburger, M. *Tetrahedron Lett.* **1996**, *37*, 3985–3988; (e) Chelucci, G.; Berta, D.; Saba, A. *Tetrahedron* **1997**, *53*, 3843–3848; (f) Hiroi, K.; Suzuki, Y.; Kawagishi, R. *Tetrahedron Lett.* **1999**, *40*, 715–718; (g) Selvakumar, K.; Valentini, M.; Pregosin, P. S. *Organometallics* **1999**, *18*, 4591–4597; (h) Hou, X.-L.; Wu, X.-W.; Dai, L.-X.; Cao, B.-X.; Sun, J. *Chem. Commun.* **2000**, 1195–1196; (i) Imai, Y.; Zhang, W.; Kida, T.; Nakatsuji, Y.; Ikeda, I. *Synlett* **1999**, 1319–1321; (j) Park, J.; Quan, Z.; Lee, S.; Han Ahn, K.; Cho, C.-W. *J. Organomet. Chem.* **1999**, *584*, 140–146; (k) Kang, J.; Lee, J. H.; Im, K. S. *J. Mol. Catal. A: Chem.* **2003**, *196*, 55–63; (l) Rassias, G. A.; Page, P. C. B.; Regnier, S.; Christie, S. D. R. *Synlett* **2000**, 379–381; (m) Tokuda, R.; Matsunaga, H.; Ishizuka, T.; Nakajima, M.; Kunieda, T. *Heterocycles* **2005**, *66*, 135–141; (n) You, S. L.; Zhou, Y. G.; Hou, X. L.; Dai, L. X. *Chem. Commun.* **1998**, 2765–2766; (o) Morimoto, T.; Tachibana, K.; Achiwa, K. *Synlett* **1997**, 783–785.
7. Selected examples: (a) Garcia Mancheno, O.; Priego, J.; Cabrera, S.; Gomez Arrayas, R.; Llamas, T.; Carlos Carretero, J. *J. Org. Chem.* **2003**, *68*, 3679–3686; (b) Enders, D.; Peters, R.; Runsink, J.; Bats, J. W. *Org. Lett.* **1999**, *1*, 1863–1866; (c) Gomez Arrayas, R.; Garcia Mancheno, O.; Carretero, J. C. *Chem. Commun.* **2004**, 1654–1655; (d) Zhang, W.; Shi, M. *Tetrahedron: Asymmetry* **2004**, *15*, 3467–3476; (e) Evans, D. A.; Campos, K. R.; Tedrow, J. S.; Michael, F. E.; Gagne, M. R. *J. Am. Chem. Soc.* **2000**, *122*, 7905–7920; (f) Khiar, N.; Suarez, B.; Valdivia, V.; Fernandez, I. *Synlett* **2005**, 2963–2967; (g) Faller, J. W.; Wilt, J. C. *Organometallics* **2005**, *24*, 5076–5083; (h) Dieguez, M.; Pamies, O.; Claver, C. *J. Organomet. Chem.* **2006**, *691*, 2257–2262; (i) Hiroi, K.; Suzuki, Y.; Abe, I.; Kawagishi, R. *Tetrahedron* **2000**, *56*, 4701–4710; (j) Nakano, H.; Takahashi, K.; Suzuki, Y.; Fujita, R. *Tetrahedron: Asymmetry* **2005**, *16*, 609–614; (k) Cheung, H. Y.; Yu, W.-Y.; Lam, F. L.; Au-Yeung, T. T.-L.; Zhou, Z.; Chan, T. H.; Chan, A. S. C. *Org. Lett.* **2007**, *9*, 4295–4298; (l) Lam, F. L.; Au-Yeung, T. T.-L.; Kwong, F. Y.; Zhou, Z.; Wong, K. Y.; Chan, A. S. C. *Angew. Chem., Int. Ed.* **2008**, *47*, 1280–1283.
8. For reviews on various ligands, see: (a) Helmchen, G.; Pfaltz, A. *Acc. Chem. Res.* **2000**, *33*, 336–345; (b) Dai, L. X.; Tu, T.; You, S. L.; Deng, W. P.; Hou, X. L. *Acc. Chem. Res.* **2003**, *36*, 659–667; (c) McManus, H. A.; Guiry, P. J. *Chem. Rev.* **2004**, *104*, 4151–4202; (d) Desimoni, G.; Faita, G.; Jorgensen, K. A. *Chem. Rev.* **2006**, *106*, 3561–3651; (e) Lu, Z.; Ma, S. M. *Angew. Chem., Int. Ed.* **2008**, *47*, 258–297; (f) Dieguez, M.; Pamies, O.; Ruiz, A.; Diaz, Y.; Castillon, S.; Claver, C. *Coord. Chem. Rev.* **2004**, *248*, 2165–2192; (g) For reviews on sulfur-containing ligands, see: Martin, E.; Diéguez, M. *C.R. Chimie* **2007**, *10*, 188–205; (h) Mellah, M.; Voituriez, A.; Schulz, E. *Chem. Rev.* **2007**, *107*, 5133–5209; (i) Masdeu-Bulto, A. M.; Dieguez, M.; Martin, E.; Gomez, M. *Coord. Chem. Rev.* **2003**, *242*, 159–201; (j) Canovese, L.; Chessa, G.; Visentin, F.; Uguagliati, P. *Coord. Chem. Rev.* **2004**, *248*, 945–954; (k) Pellissier, H. *Tetrahedron* **2007**, *63*, 1297–1330.
9. (a) Pena-Carbene, E.; Norrby, P.; Sjiegren, M.; Vitagliano, A.; De Felice, V.; Oslob, J.; Ishii, S.; Oneill, D.; Kermar, B.; Hequist, P. *J. Am. Chem. Soc.* **1996**, *118*, 4299–4313; (b) Aakermark, B.; Zetterberg, K.; Hansson, S.; Krakenberger, B.; Vitagliano, A. *J. Organomet. Chem.* **1987**, *335*, 133–142.
10. (a) Adams, H.; Anderson, J. C.; Cubbon, R.; James, D. S.; Mathias, J. P. *J. Org. Chem.* **1999**, *64*, 8256–8262; (b) Anderson, J. C.; James, D. S.; Mathias, J. P. *Tetrahedron: Asymmetry* **1998**, *9*, 753–756; (c) Tu, T.; Zhou, Y. G.; Hou, X.-L.; Dai, L. X.; Dong, X. C.; Yu, Y. H.; Sun, J. *Organometallics* **2003**, *22*, 1255–1265; (d) Hu, X. P.; Bai, C. M.; Dai, H. C.; Chen, H. L.; Zheng, Z. *J. Mol. Catal. A: Chem.* **2004**, *218*, 107–112; (e) Lopez, C.; Perez, S.; Solans, X.; Font-Bardia, M.; Roig, A.; Molins, E.; van Leeuwen, P. W. N. M.; van Strijdonck, G. P. F. *Organometallics* **2007**, *26*, 571–576.
11. (a) Allen, J. V.; Dawson, G. J.; Frost, C. G.; Williams, J. M. J. *Tetrahedron* **1994**, *50*, 799–808; (b) Sprinz, J.; Helmchen, J.; Reggelin, M.; Huttner, M.; Zsolnai, L. *Tetrahedron Lett.* **1993**, *34*, 1769–1772; (c) Dawson, G. J.; Frost, C. G.; Williams, J. M. J.; Coote, S. J. *Tetrahedron Lett.* **1993**, *34*, 3149–3150; (d) Von Matt, P.; Pflatz, A. *Angew. Chem., Int. Ed. Engl.* **1993**, *32*, 566–568; (e) Togni, A.; Venanzi, L. *Angew. Chem., Int. Ed. Engl.* **1994**, *33*, 497–526; (f) Meyers, A. Y.; Reuman, M. *Tetrahedron* **1985**, *41*, 837–860; (g) Boog-Wick, K.; Pregosin, P. S.; Trabesinger, G. *Organometallics* **1998**, *17*, 3254–3264; (h) Gomez, M.; Jansat, S.; Muller, G.; Maestro, M. A.; Mahia, J. *Organometallics* **2002**, *21*, 1077–1087; (i) Gladiali, S.; Loriga, G.; Medici, S.; Taras, R. *J. Mol. Catal. A: Chem.* **2003**, *196*, 27–38; (j) Capito, E.; Bernardi, L.; Comes-Franchini, M.; Fini, F.; Fochi, M.; Pollicino, S.; Ricci, A. *Tetrahedron: Asymmetry* **2005**, *16*, 3232–3240; (k) Takada, H.; Oda, M.; Oyamada, A.; Ohe, K.; Uemura, S. *Chirality* **2000**, *12*, 299–312.
12. (a) Chelucci, G.; Cabras, M. A. *Tetrahedron: Asymmetry* **1996**, *7*, 965–966; (b) Koning, B.; Meetsma, A.; Kellogg, R. M. *J. Org. Chem.* **1998**, *63*, 5533–5540; (c) Chelucci, G.; Bacchi, A.; Fabbri, D.; Saba, A.; Ulgheri, F. *Tetrahedron Lett.* **1999**, *40*, 553–556.
13. (a) Rassias, G. A.; Bulman Page, P. C.; Reignier, S.; Christie, S. D. R. *Synlett* **2000**, 379–381; (b) Bulman Page, P. C.; Heaney, H.; Reignier, S.; Rassias, G. A. *Synlett* **2003**, 22–28; (c) Siedlecka, R.; Wojaczynska, E.; Skarzewski, J. *Tetrahedron: Asymmetry* **2004**, *15*, 1437–1444; (d) Bernardi, L.; Bonini, B. F.; Comes-Franchini, M.; Fochi, M.; Mazzanti, G.; Ricci, A.; Varchi, G. *Eur. J. Org. Chem.* **2002**, 2776–2784; (e) Braga, A. L.; Paixao, M. W.; Milani, P.; Silveira, C. C.; Rodrigues, O. E. D.; Alves, E. F. *Synlett* **2004**, 1297–1299; (f) Anderson, J. C.; Osborne, J. *Tetrahedron: Asymmetry* **2005**, *16*, 931–934.
14. (a) Wang, M.-C.; Hou, X.-H.; Chi, C.-X.; Tang, M.-S. *Tetrahedron: Asymmetry* **2006**, *17*, 2126–2132; (b) Wang, M.-C.; Hou, X.-H.; Xu, C.-L.; Liu, L.-T.; Li, G.-L.; Wang, D.-K. *Synthesis* **2005**, 3620–3626; (c) Wang, M.-C.; Wang, D.-K.; Zhu, Y.; Liu, L.-T.; Guo, Y.-F. *Tetrahedron: Asymmetry* **2004**, *15*, 1289–1294; (d) Wang, M.-C.; Liu, L.-T.; Zhang, J.-S.; Shi, Y.-Y.; Wang, D.-K. *Tetrahedron: Asymmetry* **2004**, *15*, 3853–3859; (e) Wang, M.-C.; Zhang, Q.-J.; Zhao, W.-X.; Wang, X.-D.; Ding, X.; Jing, T.-T.; Song, M.-P. *J. Org. Chem.* **2008**, *73*, 168–176.
15. (a) Confalone, P. N.; Pizzolato, G.; Baggiolini, E. G.; Lollar, D.; Uskokovic, M. R. *J. Am. Chem. Soc.* **1977**, *99*, 7020–9026; (b) McKennon, M. J.; Meyers, A. I. *J. Org. Chem.* **1993**, *58*, 3568–3571.
16. Braga, A. L.; Appelt, H. R.; Schneider, P. H.; Silveira, C. C.; Wessjohann, L. A. *Tetrahedron: Asymmetry* **1999**, *10*, 1733–1738.
17. Willems, J. G. H.; Hersmis, M. C.; de Gelder, R.; Smits, J. M. M.; Hamink, J. B.; Dommerholt, F. J.; Thijs, L.; Zwanenburg, B. *J. Chem. Soc., Perkin Trans. 1* **1997**, 963–967.
18. Shaw, K. J.; Luly, J. R.; Rapoport, H. *J. Org. Chem.* **1985**, *50*, 4515–4523.
19. Allen, J. V.; Coote, S. J.; Dawson, G. J.; Frost, C. G.; Martin, C. J.; Williams, J. M. J. *J. Chem. Soc., Perkin Trans. 1* **1994**, 2065–2072.
20. Hayashi, T.; Yamamoto, A.; Hagihara, T.; Ito, Y. *Tetrahedron Lett.* **1986**, *27*, 191–194.
21. (a) Tsuji, J.; Takahashi, K.; Minami, I.; Shimazu, I. *Tetrahedron Lett.* **1984**, *25*, 4783–4786; (b) Carfagna, C.; Galarini, R.; Musco, A.; Santi, R. *J. Org. Chem.* **1991**, *56*, 3924–3927; (c) Saitoh, A.; Achiwa, K.; Tanaka, K.; Morimoto, T. *J. Org. Chem.* **2000**, *65*, 4227–4240.
22. Mackenzie, P. B.; Whelan, J.; Bosnich, B. *J. Am. Chem. Soc.* **1985**, *107*, 2046–2054.
23. Hayashi, T.; Yamamoto, A.; Ito, Y.; Nishioka, E.; Miura, H.; Yanagi, K. *J. Am. Chem. Soc.* **1989**, *111*, 6301–6311.
24. (a) Sweet, J. A.; Cavallari, J. M.; Price, W. A.; Ziller, J. W.; McGrath, D. V. *Tetrahedron: Asymmetry* **1997**, *8*, 207–211; (b) Togni, A.; Rihs, G.; Pregosin, P. S.; Ammann, C. *Helv. Chim. Acta* **1990**, *73*, 723–732.
25. Pregosin, P. S.; Salzmann, R. *Coord. Chem. Rev.* **1996**, *96*, 35–68.
26. (a) Aakermark, B.; Krakenberger, B.; Hansson, S.; Vitagliano, A. *Organometallics* **1987**, *6*, 620–628; (b) Macsari, I.; Hupe, E.; Szabo, K. J. *J. Org. Chem.* **1999**, *64*, 9547–9556; (c) Aranyos, A.; Szabo, K. J.; Castano, A. M.; Baeckvall, J.-E. *Organometallics* **1997**, *16*, 1058–1064; (d) Moreno-Manas, M.; Pajuelo, F.; Parella, T.; Pleixats, R. *Organometallics* **1997**, *16*, 205–209.
27. For a review on Curtin-Hammet kinetics, see: Seeman, J. I. *Chem. Rev.* **1983**, *83*, 83–134.
28. von Matt, P.; Lloyd-Jones, G. C.; Minidis, A. B. E.; Pfaltz, A.; Macko, L.; Neuburger, M.; Zehnder, M.; Rueegger, H.; Pregosin, P. S. *Helv. Chim. Acta* **1995**, *78*, 265–284.